Interpolation Methods for Time-Delay Estimation Using Cross-Correlation Method for Blood Velocity Measurement

Xiaoming Lai and Hans Torp, *Member, IEEE*

***Abstract*—The cross-correlation method (CCM) for blood flow velocity measurement using Doppler ultrasound is based on time delay estimation of echoes from pulse-to-pulse. The sampling frequency of the received signal is usually kept as low as possible in order to reduce computational complexity, and the peak in the correlation function is found by interpolating the correlation function. The parabolic-fit interpolation method introduces a bias at low sampling rate to the ultrasound center frequency ratio. In this study, four different methods are suggested to improve the estimation accuracy: (1) Parabolic interpolation with bias-compensation, derived from a theoretical signal model. (2) Parabolic interpolation combined with linear filter interpolation of the correlation function. (3) Parabolic interpolation to the complex correlation function envelope. (4) Matched filter interpolation applied to the correlation function. The new interpolation methods are analyzed both by computer simulated signals and RF-signals recorded from a patient with time delay larger than $1/f_0$, where f_0 is the center frequency. The simulation results show that these methods are more accurate than the parabolic-fit method. From the simulation, the worst estimation accuracy is about 1.25% of $1/f_0$ for the parabolic-fit interpolation, and it is improved by the above methods to less than 0.5% of $1/f_0$ when the sampling rate is 10 MHz, the center frequency is 2.5 MHz and the bandwidth is 1 MHz. This improvement also can be observed in the experimental data. Furthermore, the matched filter interpolation gives the best performance when signal-to-noise ratio (SNR) is low. This is verified both by simulation and experimentation.**

I. Introduction

Blood velocity is an important parameter for the clinical diagnosis of vascular disease. Ultrasound has become an indispensable noninvasive tool for blood velocity measurement. The pulsed wave Doppler technique is widely used because it can provide range resolution. With this method, sequential short ultrasound pulses are transmitted into the vessel or heart at a pulse repetition frequency (PRF). Return signals are received sequentially after a certain delay following the pulse transmission. Due to the movement of the scatterers, the received echo is a time-delayed version of the echo from the previous pulse if time transit effects are not considered. In the conventional autocorrelation method [1], this time shift is estimated from the pulse-to-pulse phase shift of the complex signal envelope. In the cross-correlation method (CCM) [2] and [3], the time shift of the echoes is estimated directly from the RF-signal. It has advantages over the Doppler method [4] in some circumstances. The main advantages are that CCM is a wideband estimator and it does not suffer from the Nyquist limit. The main drawback is the computational load due to RF-signal processing.

In the CCM, the time delay is estimated by searching for the maximum correlation coefficient between the successive received echoes. If the received echoes are denoted as $p(t,k)$, where t is the elapsed time after pulse transmission that corresponds to a certain depth from the transducer, k is the pulse number, its two-dimension (2-D) correlation function is denoted $R(\tau,m)$, which is defined as:

$$R(\tau,m)=\int_t\left(\sum_k p(t,k)p(t+\tau,k+m)\right)dt.$$

In the CCM, we use $R(\tau,m)$ with $m=1$ for estimating the time delay. Then the correlation function has maximum magnitude in the time delay τ_ν, i.e., $R(\tau_\nu,1)=\max_\tau R(\tau,1)$.

A 2-D correlation function model was given in [5]. The magnitude of the correlation function has a shape close to the Gaussian function [5]. With the approximated Gaussian envelope and without lateral transit time effect, a theoretical RF correlation model is:

$$R(\tau,1)=\exp\left(-\frac{(\tau-\tau_\nu)^2}{2\sigma^2}\right)\cos(2\pi f_0(\tau-\tau_\nu))$$

$$\tau_\nu=-\frac{2T\nu\cos\theta}{c}. \quad (1)$$

In which σ is the standard derivation that is related to the transmitted signal bandwidth B by $B=2/\sigma$. T is pulse repetition period, ν is the blood velocity, c is the ultrasound speed, and θ is the angle between the ultrasound beam and blood vessel. Fig. 1 is an illustration of the RF correlation function.

Manuscript received February 11, 1997; accepted August 2, 1998. This work was supported by the Norwegian University of Science and Technology, Trondheim, Norway.

X. Lai is with the Department of Medical Biophysics, Sunnybrook Health Science Centre, University of Toronto, ON Canada M4N 3M5 (e-mail: xiaoming@sten.sunnybrook.utoronto.ca).

H. Torp is with the Department of Physiology and Biomedical Engineering, The Norwegian University of Science and Technology, 7005 Trondheim, Norway.

0885–3010/99$10.00 © 1999 IEEE

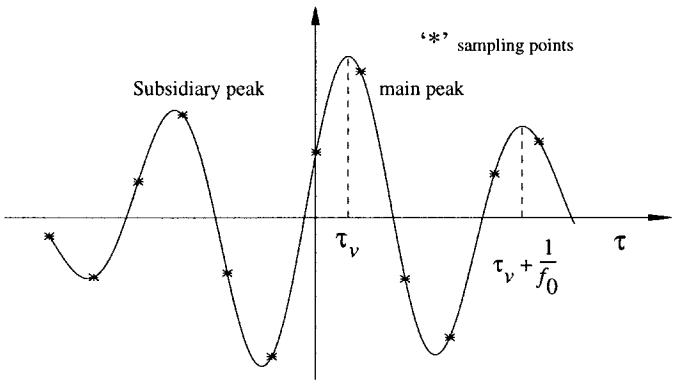

Fig. 1. RF correlation function $R(\tau, m)$ when $m = 1$.

In practice, the echo signal is discrete due to sampling in time. The true location of the maximum correlation coefficient is not constrained to discrete increments, and it may fall between the discrete sampling points that result in estimation inaccuracy. An interpolation technique usually is used to improve the time delay estimation accuracy [9]. Special interests to discuss the interpolation methods with low sampling rate are: first, the computation to calculate the correlation function and to filter the wall signal can be reduced. The received signal is usually composed of not only the blood signal but also the clutter signals or wall signal from the boundary and wall vessel; therefore, it is necessary to remove the wall signal prior to the time-delay estimation. This is generally implemented by a highpass filter or a wall filter. This filtering is performed on the signal from the same depth. When the sampling rate is lower, wall filtering calculations will be reduced. Second, most scanners use the Doppler method based on the baseband complex signal. The sampling rate is usually low in those systems. In order to implement the cross-correlation technique in those systems, the interpolation methods were investigated.

The most widely used interpolation method is the parabolic-fit that is simple, but its estimation bias is high when the sampling rate to center frequency ratio (f_s/f_0) is low (in the order of 4) [6], [9], and [11]. In addition to the parabolic-fit, the cosine-fit [7], [8], and [9] and the reconstructive interpolation methods [9] also are used. The cosine-fit interpolation can be used at $f_s/f_0 = 4$ with high estimation accuracy; but as mentioned in [7], it has velocity aliasing for velocities exceeding the Nyquist limit. The reconstructive interpolation method [9] and [10] is based on the Nyquist sampling theorem, that is, a band-limited continuous-time signal can be reconstructed from its digital samples. The key component in the reconstruction is the ideal lowpass filter. This cannot be implemented in a practical system, a reasonable approximated lowpass filter is used. Therefore, an approximated, continuous-time signal is reconstructed. Its computational time, however, is usually longer than the other interpolation methods.

In this work, four other interpolation methods are proposed and evaluated. The paper is organized as follows: In Section II, the four interpolation methods are described.

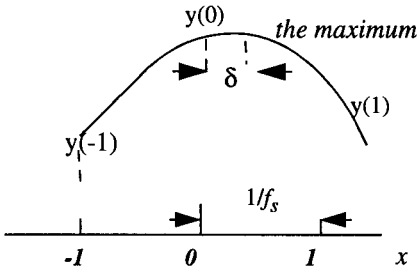

Fig. 2. An illustration of the parabolic fitting.

In Section III, the performance of the cosine-fitting interpolation method, the reconstruction filter interpolation method, and the other four interpolation methods described in Section II are compared by simulations. In Section IV, the four interpolation methods are evaluated by the experiments.

II. Interpolation Methods Description

A. Parabolic Interpolation with Bias-Compensation

Fig. 1 shows that the interpolation is necessary to get good time-delay estimation. One simple interpolation method is parabolic-fitting, which has been used in many applications. In our application, the parabolic fitting is performed near the peak and only requires a few operations. An illustration of parabolic fit is shown in Fig. 2. The parabola has the form $y(x) = ax^2 + bx + c$. The location of the maximum coefficient is:

$$\delta = -b/2a = (y(-1) - y(1))/2(y(-1) - y(0) + y(1)). \tag{2}$$

The parabolic-fit works well where the RF correlation function is sampled at a high rate, but it has substantial bias when the sampling rate is low. Specifically, it induces high bias to low Q-factor ($Q = f_0/B$) signal, which corresponds to a narrow correlation function curve. The parabolic interpolation bias also depends on the location of the time delay, or blood velocity ν. The theoretical mean and variance for a discrete signal with parabolic peak fit was derived in [11].

For a given velocity ν, the parabolic interpolation bias b is:

$$b = f\left(\nu, \frac{f_s}{f_0}, Q\right) = \nu - \hat{\nu}\left(\nu, \frac{f_s}{f_0}, Q\right) \tag{3}$$

where f is a function of argument ν, f_s/f_0, and Q; ν is the estimated velocity and $\hat{\nu}\left(\nu, \frac{f_s}{f_0}, Q\right)$ implies $\hat{\nu}$ is a function of argument ν, f_s/f_0, and Q.

If we can predict the bias b, one should be able to compensate for it by using this priori knowledge. A theoretical prediction of the bias b in our application can be obtained from the correlation function model described in (1) where the oversampling f_s/f_0 and Q-factor are given. It is

shown in Appendix 1 that in most applications, $\hat{\nu}$ and ν are uniquely determined when f_s/f_0 and Q are given. We can use a zero order approximation:

$$f\left(\nu, \frac{f_s}{f_0}, Q\right) \approx f\left(\hat{\nu}, \frac{f_s}{f_0}, Q\right). \tag{4}$$

Rewrite (3) as:

$$\nu = \hat{\nu} + b = \hat{\nu} + f\left(\hat{\nu}, \frac{f_s}{f_0}, Q\right). \tag{5}$$

The blood velocity estimated by (5) is a parabolic fit with bias compensation. Bias b is obtained from the theoretical correlation function model. The bias compensation may be implemented by a lookup table.

1. False Peaks and Aliasing: In the CCM, the velocity is estimated by the time delay, which has the maximum correlation magnitude. In practice, there may be peak hopping or false peak errors, that is, the main peak may be mistaken for subsidiary peak due to the estimation variance of the correlation function. In the Doppler method [1], there is velocity aliasing when the true velocity is beyond the Nyquist limit. The aliasing appears at a multiple of two times the Nyquist limit velocity. As discussed in [18], the false peaks in the CCM appear at time delays equivalent to a multiple of two times Nyquist velocity in the Doppler method; therefore, they are the same kind of errors in the sense of aliasing. Thus, the peak hopping or false peak detection also is called aliasing in this paper, and the velocity which corresponds to the time delay $1/2f_0$ is called the Nyquist limit.

The parabolic fit can be applied only locally around the peak. As a result, the first step in the parabolic-fit is to select the peak from the discrete correlation coefficients. Therefore, it can improve accuracy only when the global peak is correctly selected from the discrete samples. When f_s/f_0 is low, the false maximum from the subsidiary peak is selected. As a result, aliasing occurs. Aliasing occurs more frequently with the narrowband signal because its envelope of the correlation function is flat. An aliasing example is shown in Fig. 3.

2. Effect of Frequency Dependent Attenuation: In the parabolic fit with bias compensation, frequency-dependent attenuation may cause performance degradation. However, it is impractical to use the center frequency of the received signal, and in this method the center frequency of the received signal is assumed to be equal to the center frequency of the transmitted signal. Nevertheless, this does not significantly affect the estimation results because the estimated velocity bias in the parabolic fit with bias compensation is related to oversampling f_s/f_0 instead of f_0. When f_0 has a shift Δf, $f_s/(f_0 + \Delta f)$ has little difference to f_s/f_0.

3. Effect of Signal Decorrelation: The correlation function model in (1) does not include the effect of signal decorrelation. When there is serious signal decorrelation, the bias-compensation method may increase estimation bias and variance. However, in our experimentation and simulation for signals in which the lateral time transit effect has been included, the bias-compensation method still works well. No significant difference has been observed, as compared to the results of other methods.

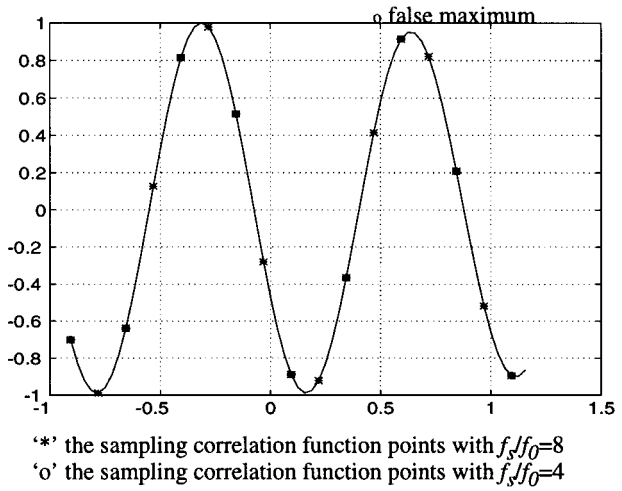

Fig. 3. An illustration that the false maximum in the discrete correlation function has occurred when the ratio of the sampling rate to the center frequency is low.

B. Parabolic-fit Interpolation Combined with Linear Filter Interpolation

The parabolic-fit interpolation uses a few correlation coefficients in the vicinity of the maximum discrete point. According to Appendix 2, the requirement for oversampling to reduce the chance of aliasing is:

$$\frac{f_s}{f_0} > \frac{\pi}{\text{acos}[\exp(-2Q^2)]}. \tag{6}$$

In many cases, this requirement is not satisfied. Increasing f_s/f_0 to Lf_s/f_0 can reduce the chance of aliasing; where L is the interpolation rate. It also reduces interpolation error by using parabolic fitting. According to (6), the required L depends on the Q-factor of the signal. For a $Q = 1$ signal, if $Lf_s/f_0 > 6.42$, there will be no aliasing induced by peak hopping error. Therefore, for a transmitted signal with an approximated two cycle period pulse (the central frequency is 2.5 MHz in our simulations later), an interpolation rate $L = 2$ is sufficient to reduce the aliasing error induced due to low oversampling $f_s/f_0 = 4$. Furthermore, the estimation bias introduced by the parabolic-fitting is small when $L = 2$. From Fig. 4, the estimation bias has been reduced when $f_s/f_0 = 4$ is increased to $f_s/f_0 = 8$.

The digital approach of the linear filter interpolation is usually used to increase the sampling rate from f_s/f_0 to Lf_s/f_0 by using a lowpass filter [10]. The process of increasing the sampling rate is described in [10] and a diagram for linear filter interpolation is plotted in Fig. 5.

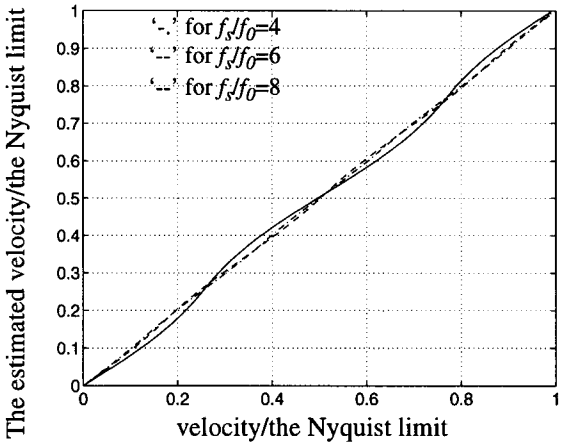

Fig. 4. The predicted mean velocity for discrete signals with parabolic-fitting.

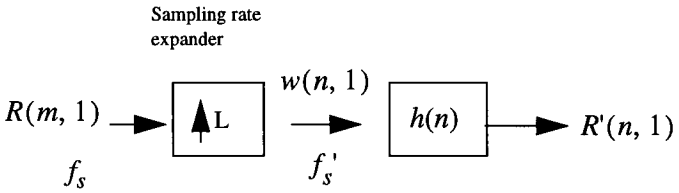

Fig. 5. Block diagram of the linear filter interpolation.

If the sampling rate f_s of the RF correlation function $R(m,1)$ is interpolated to a sampling rate f_s', $L = f_s'/f_s$, then there are $L-1$ new sample points between each pair of points of $R(m,1)$. Initially, we set these interpolation point to zero, creating the signal:

$$w(n,1) = \begin{cases} R\left(\frac{n}{L},1\right) & n = 0, \pm L, \pm 2L \dots \\ 0 & \text{otherwise} \end{cases}. \tag{7}$$

The spectrum of $w(n,1)$ contains not only baseband frequencies (i.e., $-\pi/L$ to π/L) of interest, but also the images of the baseband frequencies centered at harmonics of the original sampling frequency $(\pm 2\pi/L, \pm 4\pi/L, \dots)$. Normally, to recover the baseband signal of interest and to eliminate the unwanted image components, it is necessary to use a digital anti-aliasing filter with near an ideal lowpass characteristic:

$$H(\omega) = \begin{cases} 1 & |\omega| < \frac{\pi}{L} \\ 0 & \text{otherwise} \end{cases}. \tag{8}$$

A simple filter design, for the case $L = 2$, is by the window design method:

$$h(n) = \frac{\sin\left(\frac{\pi n}{2}\right)}{\frac{\pi n}{2}}, \quad n = 0, \pm 1, \pm 2, \dots M, \tag{9}$$

where M is the length of the window and $h(n)$ has the coefficient with:

$$h(n) = \begin{cases} 1 & n = 0 \\ 0 & n = \pm 2, \pm 4, \dots \end{cases} \tag{10}$$

This satisfies the zero-crossing criterion of ideal filters and is an efficient design where every other coefficient is zero and need not be computed in a practical implementation.

In addition to the filter in (9), other halfband filters [10] are also of interest for interpolation by a factor of two. They have a spectrum symmetric property where:

$$H(\omega) = 1 - H(\pi - \omega)$$

This also improves computation efficiency.

In this interpolation method, the sampling rate of the correlation coefficients is increased by a small factor before the parabolic fit. This is more efficient than the reconstruct filter interpolation [9] in which the interpolation rate L has to be very high ($L = 50$) to get similar estimation accuracy.

C. Parabolic Interpolation to the Complex Correlation Function Envelope

Most existing ultrasound scanners are already equipped to demodulate RF signal to the baseband signal. The sampling rate is lower in the baseband than that in RF-data. The minimum sampling rate is determined by the sampling theorem. To realize the cross-correlation technique on these scanners, the cross-correlation function is calculated and interpolated in the baseband, and then remodulated to the RF domain. It is easier to interpolate the baseband signal because it is slowly varying compared to the RF signal.

The modulation formula from baseband correlation function $R_x(\tau,k)$ to RF-band correlation function $R(\tau,k)$ [12] is:

$$R(\tau,k) = 0.5Re(R_x(\tau,k)\exp(j2\pi f_0\tau)). \tag{11}$$

From (1), the expected shape of the correlation function R_x is Gaussian shape. It is conceivable that a simple way is to parabolic fit the Gaussian function locally, that is, using several samples of the correlation function centered around its magnitude peak. An illustration of parabolic interpolation in the complex envelope is shown in the Fig. 6.

Modulation from the complex envelope to the RF correlation signal is the most costly step in terms of computation. One way to reduce computation is to modulate iteratively around the magnitude peak [9]. At each iteration, only a few points are modulated to the RF band, and the RF magnitude is compared among those points.

D. Matched Filtering for Interpolation

1. Matched Filtering for Time-Delay Estimation: Time-delay estimation is used in many applications. A generalized cross-correlation method was developed in the work [15]. The block diagram is in Fig. 7.

Due to the deteriorating effect of the noise on time delay detection, a false peak may be produced and cause a false estimate of the time delay. The purpose of the optimum linear filter is to minimize the occurrence of false peaks.

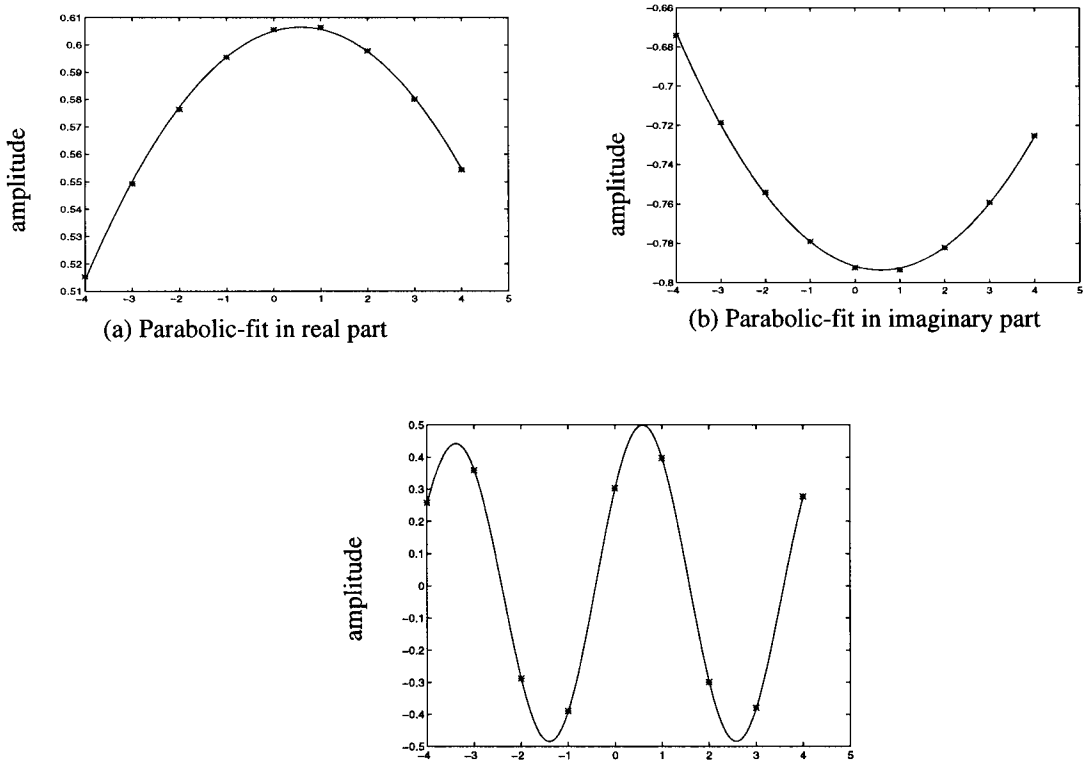

Fig. 6. An illustration of parabolic interpolation applied to the complex correlation function envelope. '$*$' is for sampled points. '-' is for the interpolated curve.

Fig. 7. Diagram of time delay estimate.

The received signal from two successive pulses is given by:

$$z(t,k) = y(t,k) + n_1(t,k) \tag{12}$$

$$z(t+\tau, k+1) = y(t+\tau, k+1) + n_2(t+\tau, k+1) \tag{13}$$

where y is the blood signal, n_1, n_2 are white Gaussian noise, and z is the received signal. The correlation function is:

$$R_z(\tau,1) = R_y(\tau,1) + R_{y,n_1}(\tau,1) + R_{n_2,y}(\tau,1) + R_{n_1,n_2}(\tau,1)$$

but due to the finite observation time, in general, $\langle R_{y,n}(\tau,1)\rangle + \langle R_{n,y}(\tau,1)\rangle$ and $R_{n_1,n_2}(\tau,1)$ are not zero, and thus contribute to the noise of the correlation function. The noise depends on the SNR of the signal and the length of the finite observation time. According to the criteria of maximizing expected signal peak at τ relative to the background noise, the resulting optimum filter [8] in terms of signal-and-noise spectral density is:

$$w(\omega) = \Phi_y(\omega) / \Phi_{n_1}(\omega)\Phi_{n_2}(\omega) + \Phi_y(\omega)(\Phi_{n_1}(\omega) + \Phi_{n_2}(\omega)) + \Phi^2 y(\omega) \tag{14}$$

where $\Phi_y(\omega)$ is the Fourier transform of the correlation function R_y and $\Phi_{n_1}(\omega)$, and $\Phi_{n_2}(\omega)$ are the noise spectral densities.

From (14), it is seen that it is certainly difficult to design the true optimum filter since it has a complicated relationship to signal and noise spectral characteristics. The Eckart filter is used in practice. It uses the criterion that maximizes the ratio of mean correlator output due to the signal present to the variance of the correlator output due to noise alone. The resulting filter is:

$$W(\omega) = \Phi_y(\omega) / \Phi_{n_1}(\omega)\Phi_{n_2}(\omega). \tag{15}$$

To the white noise, the spectral densities $\Phi_{n_1}(\omega)$ and $\Phi_{n_2}(\omega)$ are independent of ω. In this case, this suboptimal linear filter is a matched filter with impulse response $w(\tau) = R_y(\tau,1)$. The matched filter for estimating time delay is:

$$m(\tau) = \int (\hat{R}(t,1)) R_y(\tau - t, 1)\, d\tau_1 \tag{16}$$

where $\hat{R}(t,1)$ is the estimated correlation function from the signal, and $R_y(\tau,1)$ is the correlation function model. A correlation function model in which transit time effect is not taken into account is used and it is:

$$R_y(\tau,1) = \exp\left(-\frac{\tau^2}{2\sigma^2}\right)\cos(2\pi f_0 \tau). \tag{17}$$

The peak detector is performed on filtered signal $m(\tau)$.

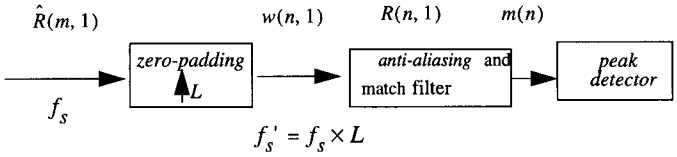

Fig. 8. Block of the match filtering and interpolation.

The optimum filter obtained in [15] was based on two conditions. One is that only two pulses have been transmitted. The other is that there is no decorrelation between the two received echoes. This is not the case here because more than two pulses have been transmitted and transverse velocity components are present. However, for simplicity, we still use the optimum filter of [15].

2. Matched Filter for Interpolation: The matched filter also can be used in the interpolation for estimation time delay when the RF-signal is sampled with a low sampling rate. The matched filter is the expected correlation function as in (17). Thus, it can be sampled according to our requirements.

In this application, the matched filter is sampled by f_s', which is rather higher than f_s and where $1/f_s'$ satisfies the resolution of the time delay estimation. This densely sampled matched filter also can be used as an anti-aliasing filter in the linear interpolation, where it is unnecessary to use an additional narrowband anti-aliasing filter. Thus, the matched filter has two functions: one is that it is a suboptimal linear filter which maximizes the signal peak to output noise; the other is that it replaces the narrowband anti-aliasing filter, which eliminates the image spectra produced in the zero padding. An implementation of the matched filter interpolation is illustrated in Fig. 8.

The correlation function is sampled by f_s. L is the interpolation rate; $w(n,1)$ is a function after $L-1$ new zero values between each pair of sample values of $\hat{R}(m,1)$ has been padded. It has the same sampling rate f_s' as the matched filter $R(n,1)$. The typical spectra is illustrated in Fig. 9.

III. Evaluating the Interpolation Methods by Simulation

The blood signal model used here is the same as in [18], where the 2-D blood signal is generated by a 2-D convolution between the echo response $h(t,k)$ from a single scatterer and a 2-D Gaussian random signal $n(t,k)$. In this model, the transit time effect in the lateral beam profile direction is included. The echo response in this simulation is:

$$h(t,k) = \exp\left(\frac{-t^2}{\sigma^2}\right)\cos(2\pi f_0 t) b(kT\nu\sin\theta)$$

where b is the transverse beam profile and it is assumed to be a Gaussian function [5]. $b(d) = \exp(-3d^2/2B^2)$ is used in our simulation, where B is the beam width. A Gaussian shape envelope in the echo response was used, as discussed in [18]. With a wideband signal, the standard deviation is set to $\sigma = 1/f_0$, giving a pulse length of approximately two cycle periods. The pulse bandwidth BW is defined as $1/\sigma$, where the magnitude of the envelope decreases by 8.69 dB.

The used parameters are given as follows: pulse repetition frequency prf, 6,564 Hz; ultrasonic measurement angle θ, 10 degree; speed of sound c, 1,540 m/s; temporal averaging ta, 1.8 ms; beamwidth, 2 mm; depth averaging ra, 2.4 μs; center frequency f_0, 2.5 MHz; bandwidth for transmitted signal, 2.5 MHz. From the above parameters, the Nyquist velocity is 1.0265 (m/s).

If the blood signal is given by $z(t,k) = y(t,k) + n_1(t,k)$, where y is the signal and n_1 is the noise, the signal-to-noise ratio for the sampled blood signals is defined as:

$$\mathrm{SNR} = 10\log\frac{\sum_n\sum_k y^2(n,k)}{\sum_n\sum_k n_1^2(n,k)}. \tag{18}$$

A. Velocity Estimation Bias and Standard Deviation by Using Different Interpolation Methods

In [16], it was indicated that the mean frequency estimate based on the correlation function has a distribution close to a Gaussian function, and the estimation variance possesses a chi-square distribution. In [18], it was shown that the CCM method and the mean frequency estimate method have the similar estimation results. Therefore, the estimation variance of the CCM method possesses a chi-square distribution. Reliability of the simulation is indicated by the 95% confidence interval. It can be obtained from the statistic [16], which is: $[0.84\mathrm{SD}, 1.25\mathrm{SD}]$ where SD is the estimated standard derivation.

Table I lists the results of velocity estimation bias and standard deviation (SD) by using different interpolation methods from 50 independent simulations. A is parabolic-fit without bias compensation. B is the cosine-fit interpolation. Method 1 is the parabolic-fit with bias-compensation. Method 2 is the parabolic-fit combined with linear filter interpolation. Method 3 is the parabolic interpolation to the complex correlation function envelope. Method 4 is the matched filter interpolation.

The results show that method 1 reduces velocity estimation bias significantly. Cosine-fit interpolation gives similar results. Because the parabolic-fit method suffers from aliasing, it is usually limited by the Nyquist limit (the time delay is within $1/2f_0$). Thus, only the estimation results to the velocities within the Nyquist limit are given in those methods.

For method 2, 3, and 4, velocities beyond the Nyquist limit, or the time delay beyond $1/f_0$ have been estimated. The results for velocities that are within the Nyquist limit are similar to the results of method 1. It should be mentioned that since method 3 operates with the demodulated signals, the sampling rate also can be reduced from 10 MHz ($f_s/f_0 = 4$) to 5 MHz ($f_s/f_0 = 2$) or even 2.5 MHz ($f_s/f_0 = 1$).

The sampling rate for the matched filter is 50 times higher than that of the signal, i.e., 500 MHz. The theoretical velocity accuracy is about 0.5% of $1/f_0$ in this case.

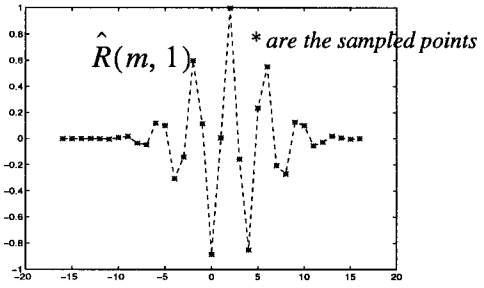

(a) The correlation function with low sampling rate

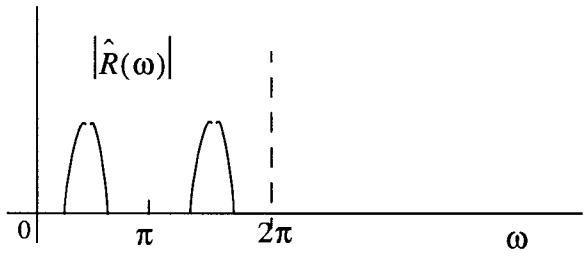

The baseband frequencies of (a)

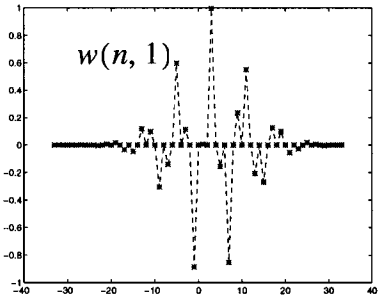

(b) The correlation function with zero padding, the sampling rate is increased from fs to fs'

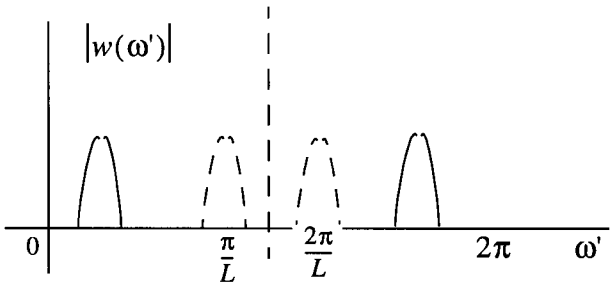

The spectrum after zero-padding which includes the baseband frequencies and their images centered at harmonics of the original sampling frequency

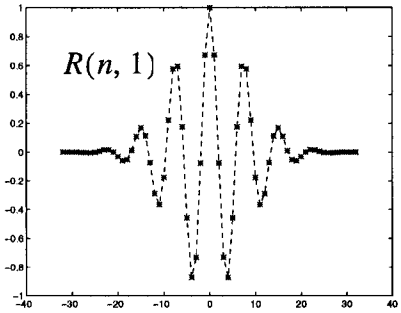

(c) The match filter with sampling rate fs'

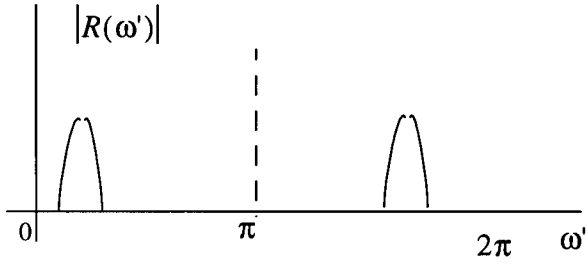

The spectra of the matched filter

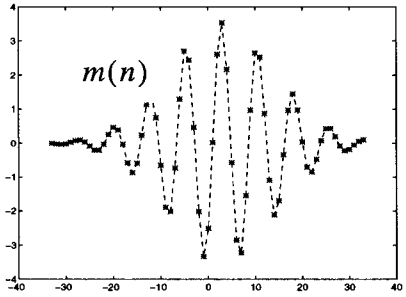

(d) The interpolated and matched correlation function

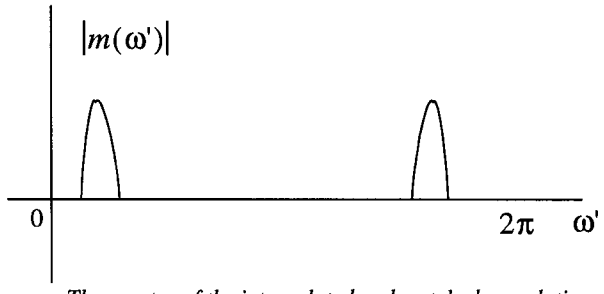

The spectra of the interpolated and matched correlation function

Fig. 9. Typical correlation function waveforms and their spectra for matched filter interpolation. Here the interpolation rate is 2.

TABLE I
VELOCITY ESTIMATION BIAS AND STANDARD DEVIATION (SD) (% NYQUIST VELOCITY) SNR = 30 dB, $f_s/f_0 = 4$.

		0.2 m/s	0.5 m/s	1.2 m/s	2.2 m/s	3.2 m/s	4.2 m/s
Bias	A	−2.1919	0.3215	—	—	—	—
	B	−0.6332	−0.0779	—	—	—	—
	Method 1	−0.0585	−0.0560	—	—	—	—
	Method 2	−0.3082	−0.5832	0.4834	0.5210	0.7866	0.3295
	Method 3	−0.093	−0.049	0.097	0.010	0.195	0.023
	Method 4	0.434	0.591	0.818	0.880	0.721	0.418
SD	A	1.2859	1.1593	—	—	—	—
	B	1.0619	1.4126	—	—	—	—
	Method 1	1.0326	1.4189	—	—	—	—
	Method 2	1.1412	1.4588	1.8770	1.9351	2.5188	3.0802
	Method 3	0.922	1.442	1.724	1.812	2.289	2.871
	Method 4	1.007	1.474	1.841	1.938	2.565	3.079

The results show that there is no significant difference to the results of methods 2 and 3.

B. Performance Comparison Between the Interpolation Methods in the Low Signal-to-Noise Ratio Circumstance

As mentioned previously, due to the deteriorating effect of noise on the time delay detection, a false peak in the correlation function may have appeared. This leads to a wrong estimation. The simulation in this section shows that the probability for wrong peak detection is reduced by using the matched filter method.

The four interpolation methods mentioned in this paper are applied to the simulation signal for $Q = 3$ and SNR $= -6$ dB for comparison. The length of the transmitted pulse is approximately six cycle periods. In this case, the required interpolation rate L for method 2 is 5 according to (6).

The results are from 900 simulations. The velocities vary from 0.1 m/s to 0.9 m/s in interval of 0.1 m/s (the Nyquist limit is 1.0265 m/s). In this simulation, the velocity estimation range has not been limited for method 1. The purpose is to display the aliasing error due to low oversampling.

Histograms for velocity estimation bias are plotted as in Fig. 10. The distribution of the bias around zero shows the velocity estimation variance. Due to aliasing, some estimates were distributed around twice the Nyquist limit, which corresponds the time delay $1/f_0$.

From the simulation results, the matched filter gives best performance at low SNR. This improvement is even more significant for narrow bandwidth signals because the matched filter is more efficient in removing noise in the narrow band cases.

C. Computation Comparison

To implement the CCM method, the received RF data needs to pass through a high-pass filter prior to the correlation function calculation. The computation requirements are usually high when the sampling rate is high, due to filtering and correlation function calculations. Table II gives approximated number of multiplication operations for $f_s/f_0 = 8$ with the parabolic interpolation method and $f_s/f_0 = 4$ with the four new interpolation methods. All the methods listed in Table II give similar estimation accuracy; however, the number of operations required for the case $f_s/f_0 = 4$ is reduced.

In Table III, we assume that a regression filter is used as a high pass filter [19] and the number of operations needed for the high pass filter is $2(p+1)K$ [20] in which p is the order of the regression filter, and K is number of samples in the temporal direction. The number of operations required for the correlation function calculation is assumed to be proportional to data block size $N * K$, where N is number of samples in the depth direction.

When $f_s/f_0 = 8$, the parabolic interpolation method is used and only one division is required as in (2). When $f_s/f_0 = 4$, interpolation method 1 uses parabolic fitting followed by a look-up table for compensation. Only one division is needed in this interpolation method.

In interpolation method 2, we interpolate the correlation function $R(n, 1)$ by a small rate using a linear filter interpolation method. In our simulation, we used a half-band filter and the number of operations for this linear filter interpolation is 51.

In interpolation method 3, we have to modulate the complex signal to the RF domain. This is a time-consuming process. In order to save the computation time, we modulate some samples and choose the global maximum. Then we use iteration around the maximum samples. At each iteration, only two samples are modulated. In our simulation, total number of operations for this interpolation method is 88.

In interpolation 4, the computation requirements are usually high for the high interpolation rate. To save the computation time, we used a method similar to the interpolation method 3. In our simulation, the number of operations is 748. A summary of the number of operations is in Table III. The histogram in Fig. 11 shows the difference of the number of operations for the case when $N = 48$ ($f_s/f_0 = 8$), $K = 32$, and $p = 3$.

The number of operations is reduced when f_s/f_0 is reduced to 4. Furthermore, the number of operations can

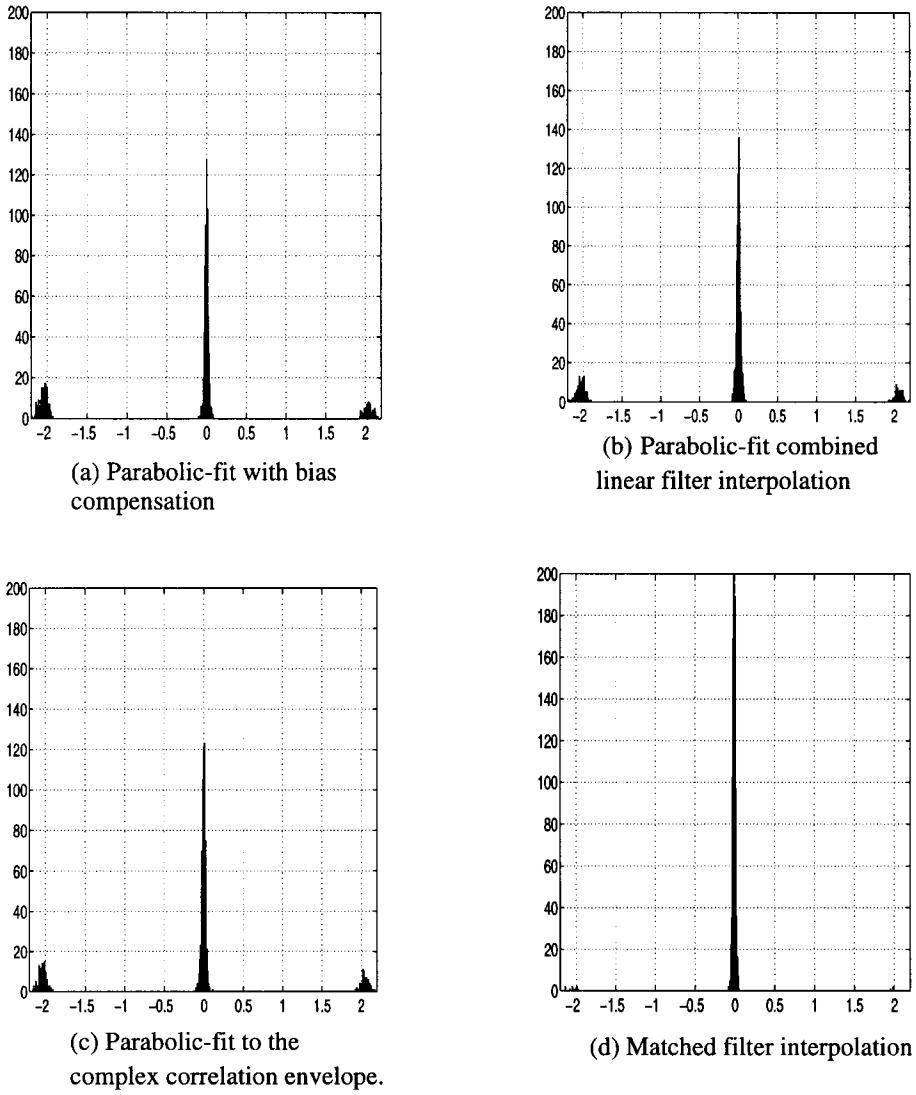

Fig. 10. Histograms (from 900 simulations) for velocity estimation bias with simulation signal $Q = 3$ and SNR $= -6$ dB.

TABLE II
SUMMARIZES THE CHARACTERISTICS OF THE INTERPOLATION METHODS.

	Method 1[1]	Method 2	Method 3	Method 4
Perform on RF or baseband signal	RF-band	RF-band	Baseband	RF-band
Oversampling f_s/f_0	$f_s/f_0 = 4$	$f_s/f_0 = 4$	$f_s/f_0 = 1, 2, 4$	$f_s/f_0 = 4$
Estimation error	Small	Small	Small	Small
Velocity estimation range	Within the Nyquist limit	Excess the Nyquist limit	Excess the Nyquist limit	Excess the Nyquist limit
Computation time	Short	Medium	Medium	Long
Using a priori information of the theoretical correlation model	Yes	No	No	Yes
Performance for low SNR	Not good	Not good	Not good	Best

[1]Method 1: parabolic fit with bias compensation, method 2: parabolic fit combined with linear filter interpolation, method 3: parabolic fit to the complex correlation envelope, method 4: matched filter interpolation.

TABLE III
A COMPARISON OF THE NUMBER OF OPERATIONS FOR DIFFERENT INTERPOLATION METHODS.

	$f_s/f_0 = 8$	$f_s/f_0 = 4$			
	Parabolic-fitting	Method 1	Method 2	Method 3	Method 4
Wall filter	$N(p+1)K$	$N(p+1)K/2$			
Correlation function	$N*K$	$NK/2$			
Interpolation	1	1	51	88	748
Total for case $N = 48$, $K = 32$, and $p = 3$	7,681	3,841	3,891	3,928	4,588

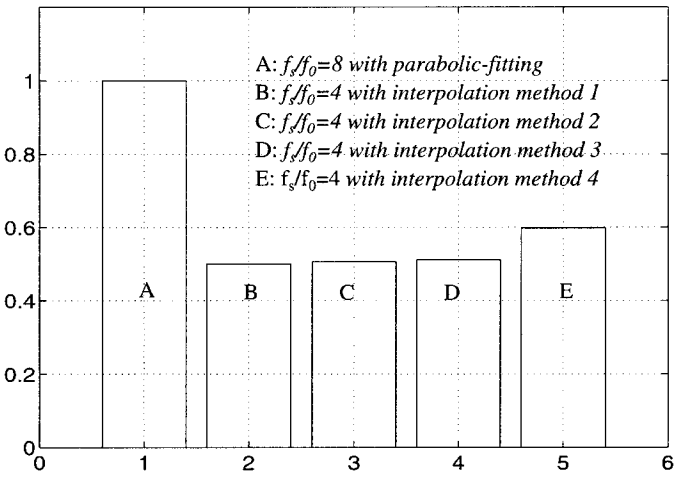

Fig. 11. A comparison of the number of operations for different interpolation methods.

be reduced significantly when the original f_s/f_0 is higher than 8.

D. Summary the Simulation Results

From simulation results, when the true velocity is within the Nyquist limit, method 1 gives similar performance to other interpolation methods, and it has a shortest computation time. Methods 2, 3, and 4 give good results, up to 4 times the Nyquist limit. Method 4 gives the best performance when the signal-to-noise ratio is low. Table II summarizes the characteristics of the interpolation methods. The choice of the interpolation method depends mainly on the specific application.

IV. Experimental Evaluation

The interpolation methods are verified by experimental data from the human subclavian artery. The RF data from a ultrasound scanner (CFM 800, Vingmed Sound AS, Norway) was collected in real time via a custom data acquisition system. The slow tissue movement signal in the raw data was removed by a 4th order IIR butterworth high pass filter with normalized cutoff frequency 0.155. Then the data was demodulated with center frequency 2.5 MHz.

A. The Parabolic Interpolation with Bias-Compensation Applied to Experimental Data with the Velocities Within the Nyquist Limit

The parameters in this experiment were the same as in the simulations. When method 1 is applied to the signal with $f_s/f_0 = 4$, aliasing often occurs. Thus, we only applied this method to a set of experimental data with velocities within the Nyquist limit. The experimental results from the subclavian artery are shown in Fig. 12. The cosine-fit method also is applied to the same experimental data for comparison.

Method 1 has significantly improved the estimation result. There is no significant difference between method 1 and the cosine-fit interpolation method.

B. The Interpolation Methods Applied to the Experimental Data with Velocities Beyond the Nyquist Limit

Experimental data from the subclavian artery with velocities up to twice the Nyquist limit were obtained. In the experiment, the oversampling $f_s/f_0 = 4$. The results in Figs. 13 and 14 show that methods 2, 3, and 4 can interpolate the correlation function with velocities beyond the Nyquist limit. From Figs. 14(a), (b), and (c), (c) has fewest velocity aliasing errors. Because the Q-factor in this experiment data is only 1, the performance improvement of the matched filter interpolation is not as significant as that in the simulation where Q is 3.

In Fig. 14, velocity aliasing errors can be seen. This is due to the fact that factors such as depth averaging time and temporal averaging time, correlation function estimator, and signal-to-noise ratio, all can affect the estimation variance of the correlation function. Furthermore, the performance of the interpolation methods are somewhat limited by the use of decimation of the RF signal to achieve the low sampling rate in the experimental evaluation because the Doppler signal is usually not a narrow band-limited signal. As a consequence, the likely performance of the estimator will be poorer than shown in the simulation. The matched filter method can reduce only the velocity aliasing error caused by low signal-to-noise ratio. Aliasing can be further reduced by a 2-D tracking method. It is based on the knowledge from flow physics that the blood velocity is continuous both in depth and temporal directions, while aliasing makes the velocity discontinu-

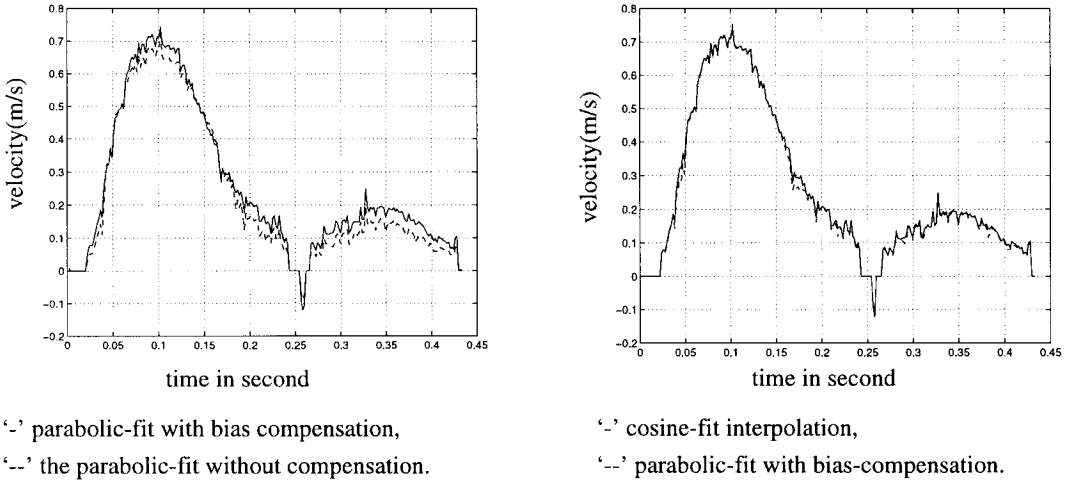

Fig. 12. Experimental evaluation of parabolic fit with bias compensation, parabolic-fit and cosine-fit interpolation methods.

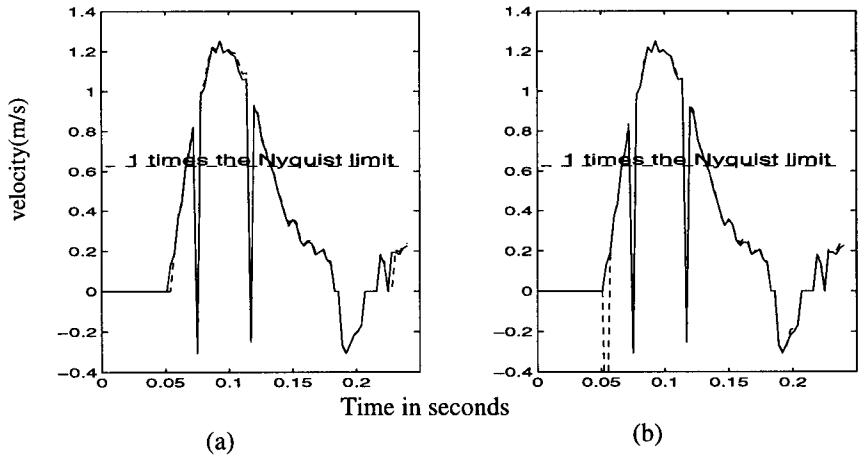

Fig. 13. Experimental evaluation: methods 2, 3, and 4 applied to the experimental data with velocities beyond the Nyquist limit. The '--' in (a) parabolic-fit to the complex correlation envelope, '–' in (a) and (b) matched filter interpolation, '--' in (b) parabolic-fit combined with linear filter interpolation.

ous. When a velocity discontinuity in the velocity image is detected, twice the Nyquist velocity should be added or subtracted until the difference between its velocity and the velocity of neighboring points is within the Nyquist limit. The velocity image after 2-D tracking is shown in Fig. 14(d). This 2-D tracking is sensitive to the selection of start point. It cannot work well when there are too many aliasing errors. Therefore, the aliasing should be reduced as much as possible before applying 2-D tracking.

V. Conclusions

Four interpolation methods for time delay estimation in the RF-signal cross-correlation technique for blood velocity measurement are presented. All the methods have higher velocity estimation accuracy than the parabolic fit when f_s/f_0 is 4. The estimation accuracy is improved from 1.25% to 0.5% of $1/f_0$ compared to the parabolic fit interpolation method when $f_s/f_0 = 4$ and $Q = 1$.

The first method, parabolic fit with bias-compensation, has shortest computation time, but suffers from aliasing at low oversampling. It works well if the velocity range is limited within the Nyquist limit that corresponds to the time delay $1/2f_0$.

The second method, parabolic fit combined with linear filter interpolation, avoids much aliasing by interpolating the correlation function at a higher sampling rate. Its computation time is between methods 1, 3, and 4.

The third method, parabolic fit to the complex correlation function envelope, performs as well as method 2, but requires intensive computations modulating the baseband signal to the RF-band. An iterative approach can reduce computation time greatly.

The fourth method, matched filter interpolation, maximizes the expected peak value relative to noise. Therefore, it has the best performance when SNR is low. This performance improvement is more significant for narrow-band signals.

The interpolation methods were verified by simulations with velocities up to four times the Nyquist limit corresponding to the time delay $2/f_0$. Further verification was

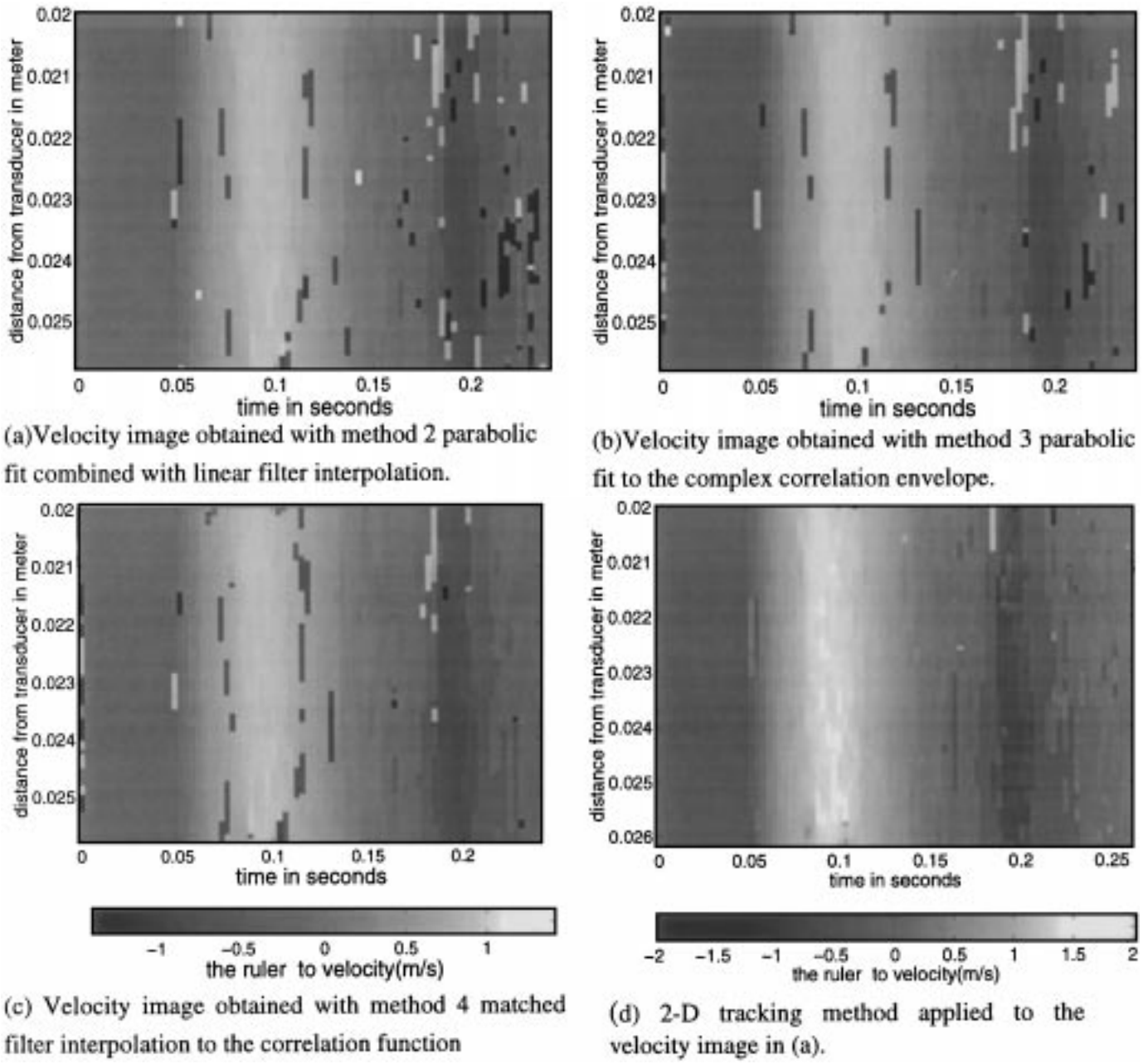

(a)Velocity image obtained with method 2 parabolic fit combined with linear filter interpolation.

(b)Velocity image obtained with method 3 parabolic fit to the complex correlation envelope.

(c) Velocity image obtained with method 4 matched filter interpolation to the correlation function

(d) 2-D tracking method applied to the velocity image in (a).

Fig. 14. Velocity image of the subclavian artery with the velocities up to twice the Nyquist limit.

provided by in vivo measurements in a subclavian artery with velocities up to four times the Nyquist limit. Velocity images have been obtained using methods 2, 3, and 4. Most pixels seem to display the correct velocities, but a small number of pixels still demonstrate aliasing. A 2-D tracking was used to further reduce aliasing.

Acknowledgment

The authors would like to thank Mr. Chien Ting Chin, and Mr. Norman Freeman at the Department of Medical Biophysics Sunnybrook, Health Science Centre, University of Toronto, Canada, for reading and correcting this work. The authors also wish to express their appreciation to the anonymous reviewers.

Appendix 1

The explanation for the unique determined relation of v and ν: from Fig. 4 [6] and [11], the predicted velocity bias b can be approximated by:

$$\hat{\nu} = \nu - b = \nu - p \sin \frac{N}{200} \pi \nu \tag{19}$$

where p is the maximum magnitude of the estimation bias. $N = f_s/f_0$ is oversampling, ν is the true velocity in terms of percent of the Nyquist limit.

The first order derivative with respect to ν is:

$$\hat{\nu}' = 1 - p \frac{N}{200} \pi \cos \frac{N}{200} \pi \nu \tag{20}$$

when $p\frac{N}{200}\pi < 1$, i.e.:

$$pN < \frac{200}{\pi} \tag{21}$$

then ν' is strictly positive, and it is a monotonic function of ν; (21) usually is true, for instance, $pN = 2.5 \times 4 < \frac{200}{\pi}$ for the signal with $Q = 1$ shown in Fig. 4.

Appendix 2

The requirement of oversampling to reduce likelihood of aliasing in the curve fitting : Considering the correlation function $R(\tau, 1)$ and its sampled version $R\left(\frac{n}{f_s}, 1\right)$, if the true time delay τ_ν happens to lie midway between two sampled points and a subsidiary peak lies on a sampled point, the possibility exists that the sample point of the subsidiary peak has a higher value than the point of the true peak, causing aliasing (refer to Figs. 1 and 3). In the worst case, we have sample points at $\tau_\nu \pm \frac{1}{2f_s}$ (half sampling period on both sides of τ_ν) and at $\tau_\nu \pm \frac{1}{f_0}$ (the two nearest subsidiary peaks on both sides of τ_ν). Aliasing occurs when:

$$R\left(\tau_\nu + \frac{1}{2f_s}, 1\right) \leq R\left(\tau_\nu + \frac{1}{f_0}, 1\right). \tag{22}$$

Assuming the correlation function model (1), then (22) becomes:

$$\exp\left(-\frac{\left(\frac{1}{2f_s}\right)^2}{2\sigma^2}\right)\cos\left(\frac{2\pi f_0}{2f_s}\right) \leq \exp\left(-\frac{\left(\frac{1}{f_0}\right)^2}{2\sigma^2}\right). \tag{23}$$

Because f_s is usually high compared to $\frac{1}{\sigma}$, we use the approximation:

$$\exp\left(-\frac{\left(\frac{1}{2f_s}\right)^2}{2\sigma^2}\right) \approx 1. \tag{24}$$

Then (23) can be written as:

$$\cos\left(\frac{\pi f_0}{f_s}\right) \leq \exp(-1/2(\sigma f_0)^2). \tag{25}$$

The required oversampling to reduce likelihood of aliasing is:

$$\frac{f_s}{f_0} > \frac{\pi}{\operatorname{acos}[\exp(-1/2(\sigma f_0)^2)]} = \frac{\pi}{\operatorname{acos}[\exp(-2Q^2)]}. \tag{26}$$

References

[1] C. Kasai, K. Namekawa, A. Koyano, and R. Omoto, "Real-time two-dimensional blood flow imaging using an autocorrelation technique," *IEEE Trans. Sonics Ultrason.*, vol. SU-32, pp. 458–464, 1985.

[2] O. Bonnefous and P. Pesque, "Time domain formulation of pulse-doppler ultrasound and blood velocity estimation by cross-correlation," *Ultrason. Imag.* 1986, pp. 73–85.

[3] O. Bonnefous, P. Pesque, and X. Bernard, "A new velocity estimator for color flow mapping," *Proc. IEEE Ultrason. Symp.*, 1986, pp. 885–860.

[4] I. A. Hein and W. D. O'Brien, "Current time-domain methods for assessing tissue motion by analysis from reflected ultrasound echoes—A review," *IEEE Trans. Ultrason., Ferroelect., Freq. Contr.*, vol. 40, Mar. 1993, pp. 84–102.

[5] H. Torp, K. Kristoffersen, and B. Angelsen, "Autocorrelation technique in color flow imaging, signal model and statistical properties of the autocorrelation estimates," *IEEE Trans. Ultrason., Ferroelect., Freq. Contr.*, vol. 41, Sep. 1994, pp 604–612.

[6] G. T. C. Foster, M. P. Embree, and W. D. O' Brien, "Flow velocity profile via time-domain correlation: Error analysis and computer simulation," *IEEE Trans. Ultrason., Ferroelect., Freq. Contr.*, vol. 37, pp. 164–174, 1990.

[7] P. G. M de Jong, T. Arts, A. P. G. Hoeks, and R. S Reneman, "Determination of tissue motion velocity by correlation interpolation of pulsed ultrasonic echo signals," *Ultrason. Imaging*, vol. 12, pp. 84–98, 1990.

[8] ——, "Experiment evaluation of the correlation interpolation technique to measure regional tissue velocity," *Ultrason. Imaging*, vol. 13, pp. 145–161, 1991.

[9] I. Cespedes, Y. Huang, J. Ophir, and S. Spratt, "Method for estimation of subsample time delays of digitized echo signals," *Ultrason. Imaging*, vol. 17, pp. 142–171, 1995.

[10] J. S. Lim and A. V. Oppenheim, *Advanced Topics in Signal Processing*. Englewood Cliffs, NJ: Prentice-Hall, 1988.

[11] R. E. Boucher and J. C. Hassab, "Analysis of discrete implementation of generalized cross correlator," *IEEE Trans. Acoust., Speech, Signal Processing*, vol. ASSP-29, no. 3, June 1981, pp. 609–611.

[12] H. Torp, X. M. Lai, and K. Kristoffersen, "Comparison between cross-correlation and auto-correlation technique in color flow image," in *Proc. IEEE Int. Ultrason. Symp.*, Baltimore, MD, 1993, pp. 1039–1042.

[13] H. Torp and K. Kristoffersen, "Velocity matched spectrum analysis: A new method for suppressing velocity ambiguity in pulsed-wave Doppler," *Ultrason. Med. Biol.*, vol. 21, no. 7, pp. 937–944, 1995.

[14] K. W. Ferrara, V. R. Algaz, and J. Liu, "The effect of frequency dependent scattering and attenuation on the estimation of blood velocity using ultrasound," *IEEE Trans. Ultrason., Ferroelect., Freq. Contr.*, vol. 39, Nov. 1992, pp. 754–767.

[15] J. C. Hassab and R.E. Bouchek, "Optimum estimation of time delay by a generalized corrector," *IEEE Trans. Acoust., Speech, Signal Processing*, vol. ASSP-27, pp. 373–380, Aug. 1979.

[16] E. R. Dougherty, *Probability and Statistics for the Engineering, Computing and Physical Sciences*. Englewood Cliffs, NJ: Prentice-Hall, 1990, Ch. 7, pp. 309–373.

[17] K. W. Ferrara and V. R. Algazi, "A new wideband spread target maximum likelihood estimator for blood velocity estimation—Part I: Theory," *IEEE Trans. Ultrason., Ferroelect., Freq. Contr.*, vol. 38, Jan. 1991, pp. 1–26.

[18] X. Lai, H. Torp, and K. Kristoffersen, "An extended autocorrelation method for estimation of blood velocity," *IEEE Trans. Ultrason., Ferroelect., Freq. Contr.*, vol. 44, no. 6, pp. 1332–1342, Nov. 1997.

[19] H. Torp, "Clutter rejection filters in color flow imaging: A theoretical approach," *IEEE Trans. Ultrason., Ferroelect., Freq. Contr.*, vol. 44, Mar. 1997, pp. 417–424.

[20] A. Kadi and T. Loupas, "On the performance of regression and step-initialized IIR clutters for colour Doppler systems in diagnosing medical ultrasound," *IEEE Trans. Ultrason., Ferroelect., Freq. Contr.*, vol. 42, no. 5, pp. 927–937, 1995.

Xiaoming Lai was born in Hunan, China, in 1965. She received the B.S. and M.S. degrees from Huazhong University of Science and Technology, Wuhan, China, in 1986 and 1989, respectively. From 1989 to 1991 she worked as an assistant engineer in the communication department, Huazhong Electronic Power Administration Company, Wuhan, China. She received the Ph.D degree in 1998 in the Department of Biomedical Engineering and Department of Engineering Cybernetics at Norwegian University of Science and Technology, Trondheim, Norway. Since 1997, she has been working in the Department of Medical Biophysics, Sunnybrook Health Science Centre, University of Toronto, Ont, Canada M4N 3M5 (e-mail: xiaoming@sten.sunnybrook.utoronto.ca) as a research engineer. Her research areas include signal processing and analysis with application in ultrasound Doppler imaging system.

Hans Torp (M'92) was born in Sarpsborg, Norway, in 1953. He received the M.S. and Dr.Techn. degrees from the University of Trondheim, Norway, in 1978 and 1992, respectively. From 1979 to 1983 he worked at the Division of Automatic Control, SINTEF (The foundation of Scientific and Industrial Research) in Trondheim. Since 1983 he has been working at the Department of Physiology and Biomedical Engineering, Faculty of Medicine, Norwegian University of Science and Technology, Trondheim, Norway. He currently is a research fellow, holding a stipend from the Norwegian Research Council.

His research areas include stochastic signal/image processing with applications in ultrasonic imaging, Doppler, and color flow imaging.